The Association Of Radiographers Of Nigeria
EYE OF MEDICINE

JOURNAL OF RADIOGRAPHY & RADIATION SCIENCES

ISSN: 1115- 7976 Vol 32, Issue 1, May 2018

The Official Journal of The Association of Radiographers of Nigeria

J R R S

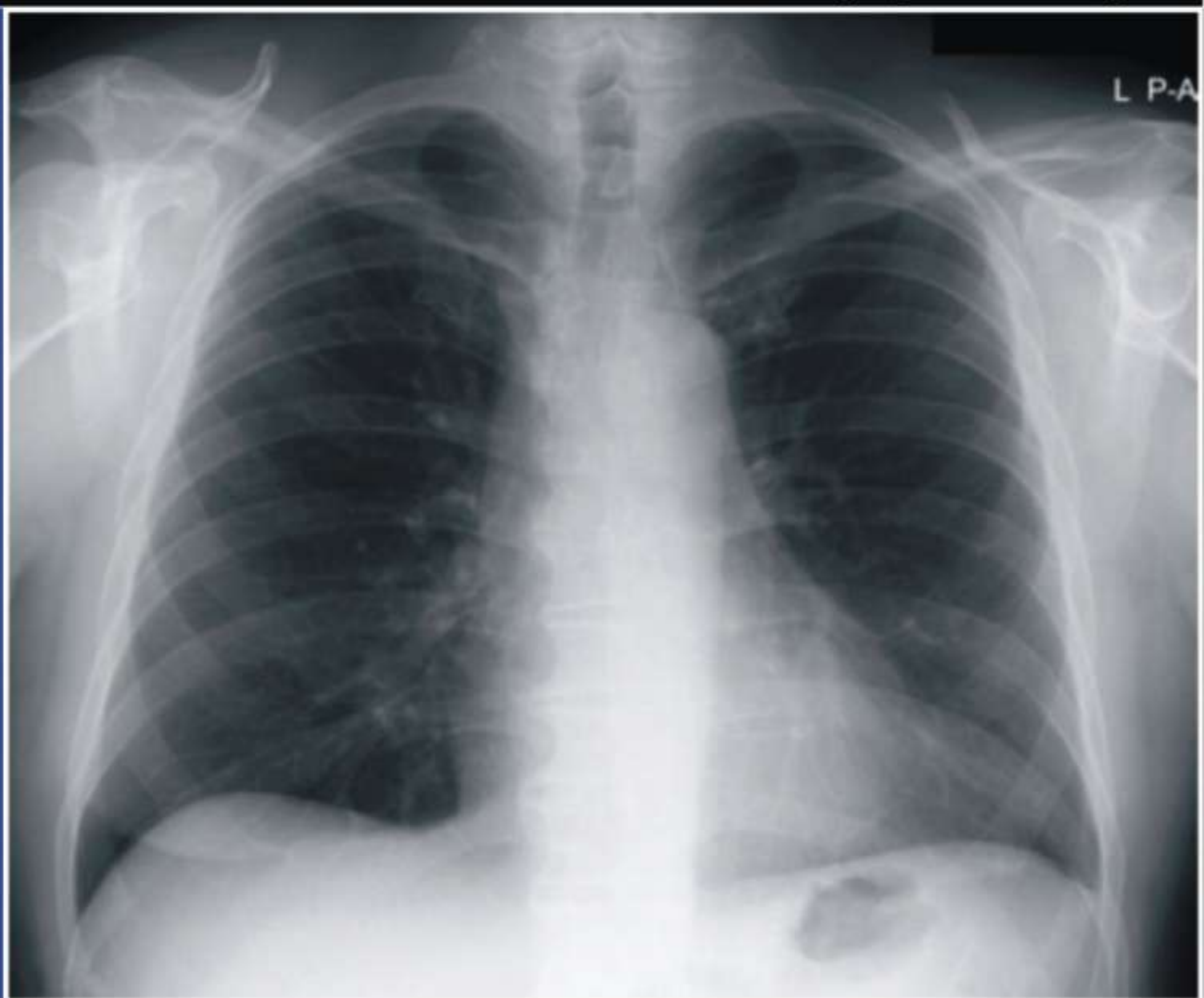

Journal homepage: www.jarnigeria.com

Development and Optimisation of Surface and Volume Radiofrequency Coils Suitable for Fast-Field-Cycling Magnetic Resonance Imaging (FFC-MRI)

***Umar Abubakar [1], Lionel Broch[2], Chukwuka Anthony Ugwu[3], Sadiq Abubakar Audu[1], Mohammed Danfulani[4], Abacha Mohammed[1], Mohammed Abba[5], Nike Mutiat Miftaudeen[6]**

[1]Department of Radiography, Usmanu Danfodiyo University, Sokoto, Nigeria

[2]Department of Medical Imaging and Medical Physics, University of Aberdeen, Scotland, United Kingdom

[3]Department of Radiography & Radiological Sciences, Nnamdi Azikiwe University, Nnewi Campus, Nigeria

[4]Department of Radiology, Usmanu Danfodiyo University, Sokoto, Nigeria

[5]Department of Medical Radiography, Bayero University, Nigeria

[6]Department of Radiotherapy, Usmanu Danfodiyo University Teaching Hospital, Sokoto, Nigeria

***Corresponding author:** umar.abubakar5@udusok.edu.ng; +2348062847518

Received: 18 February 2018. Received in revised form: 18 April, 2018. Accepted: 25 April, 2018

ABSTRACT

Objective: To evaluate a modelling and design methodology employed in constructing and optimizing radiofrequency (RF) coils suitable for use with the whole-body fast-field-cycling Magnetic Resonance Imaging (FFC-MRI). It is also aimed at comparing the sensitivity and the signal-to-noise ratio (SNR) of the various types of surface RF coils constructed at the initial and final stages of this research.

Methodology: An experimental study carried out at Biomedical MRI Laboratory at University of Aberdeen. Various designs of RF coil were constructed, optimized and tested with network/signal analyser for use with an experimental FFC - MRI scanner, operating at a detection magnetic field of 0.2 T (proton Larmor frequency of 8.5 MHz). The coils comprised circular loop (CL) RF – receive surface coil and a birdcage RF – transmit volume coil. The intrinsic parameters of the CL coils were measured using a search-coil field probe and a network/signal analyser.

Results: The CL surface coil constructed with copper wire had resonant frequency of 8.46 MHz and Quality factor (Q – factor) of 47.1 while the resonant frequency of the one constructed with litz wire was 8.54 MHz and Q - factor of 85.4 MHz. The intrinsic parameter of the birdcage volume coil was 8.48 MHz and Q - factor of 102.

Conclusion: Bench testing of the coils showed promise as receiver and transmit coils for the FFC-MRI system

Keywords: Fast field cycling MRI, Circular Loop Coil, Birdcage coil, Q- factor

Introduction

Magnetic Resonance Imaging is a diagnostic imaging technique based on the emission of electromagnetic waves from the body when the patient is placed in a strong magnetic field andexposed to radiofrequency radiation [1]. This is achieved through the magnet that generates a strong, constant magnetic field, radiofrequency transmit and receive coils which excite and detect nuclear magnetic resonance (NMR) signals, and magnetic field gradients, which localizes the NMR signal [2].

Fast Field Cycling (FFC) MRI is a special type of MRI scanner which allows switching of the magnetic field during image acquisition. This differs from the MRI approach that produces a constant magnetic field during the scan [3]. The rationale behind this technique is to produce endogenous contrast of the patient under examination by measuring the pattern of variations of T_1 relative to magnetic field [4]. This new type of MRI technique is more sensitive to pathological changes in tissues when compared to conventional MRI scanner [5].

An FFC-NMR pulse sequence is composed of three distinct periods called 'polarization', 'evolution' and 'detection', and each of these periods have their own distinct value of applied magnetic field (Figure 1) [6]. The switching of this magnetic field during pulse sequences enables the nuclear spins to 'evolve', and the applied magnetic field strength during this period can be changed, but if the magnetic field is switched to a "detection" period, the applied magnetic field strength is always constant, in order to have an NMR signal with uniform frequency [7].

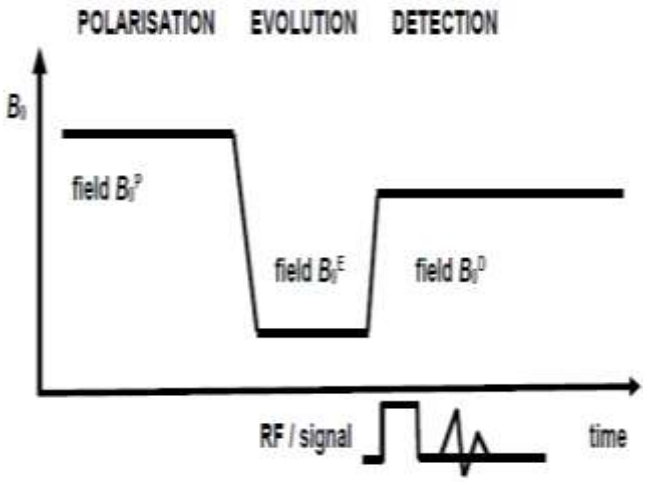

Figure 1: The pulse sequence of field-cycling, showing the three periods. Relaxation occurs during the evolution period, while signal detection takes place during detection period.

The Inversion Recovery (IR) sequence allows the sample to pre-polarise in the $\boldsymbol{B_0^P}$ field, then switched to B_0^D where the pre-polarised magnetisation is inverted following the application of the first 180^0 RF pulse. The sample will now relax when the magnet is switched to B_0^E for a variable period.

Finally, the field is switched to B_0^D field where a 90^0 RF pulse is applied to generate the FID and the acquisition of images (Figure 2) [5, 6].

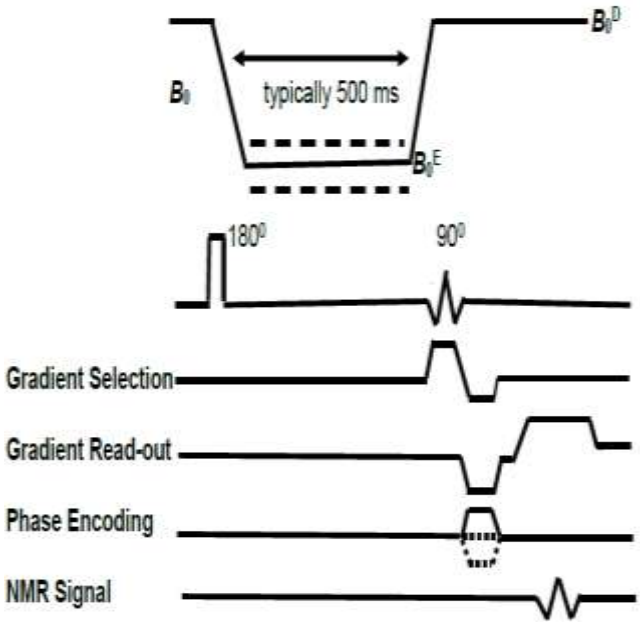

Figure 2: Fast-field-cycling inversion-recovery pulse sequence for relaxometric imaging measurements.

The radiofrequency (RF) system consists of a transmitter and a receiver coil. The RF pulses are generated by a whole body excitation transmitter coil responsible for the MR signals, that provides diagnostic information produced within the patient's tissue [8].

The Receiver Surface Coil

After the tipping of the magnetisation vector (M) to the transverse component (M_{XY}), it will continue precessing at Larmor frequency, $\boldsymbol{\omega_L}$, and a voltage known as electromotive force (EMF) will be induced across the ends of the coil. This process is called Faraday induction (Figure 3) [9].

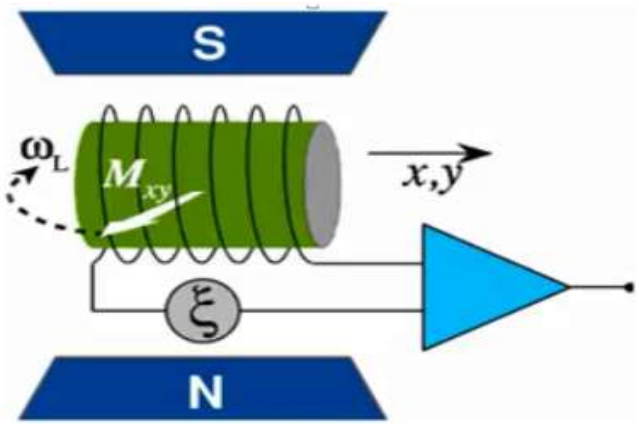

Figure 3: Schematic of a receiver and a receive amplifier connected to it.

The voltage (EMF) can be expressed as:

Voltage (EMF): $|\xi| = \omega\Phi_a$ (equation 1)

Where Φ_a is the magnitude of the rotating flux. From the expression above, it means that when the B_0 field is increased, then the precessional frequency ω_L will also increase likewise the induced signal voltage.

Over the years, a great number of MRI, FFC - MRI and MR Spectroscopy (MRS) studies have employed a variety of RF surface coils [10,11], including double-tuned coil designs [12]. In recent years, specially designed RF phased-arrays, composed of a number of surface RF coils, have been used to increase the SNR [13, 14] or to reduce the acquisition time by means of parallel imaging techniques [15].

The simplest, and most used, RF surface coil design consists of a circular or rectangular loop, giving a B_1 field that in the central region of the coil is perpendicular to the coil plane (axial RF field) [16]. This RF coil design is especially suitable for MRI systems with horizontal B_0 field and a great number of FFC - MRI pre-clinical and clinical applications have been demonstrated [17].

The Transmitter Volume Coil

The transmitter generates the RF field, $\boldsymbol{B_1}$, required to tip the magnetisation vector (M) from its equilibrium to the transverse component. The amplifier, which is connected to the end of the coil drives an oscillating current, I_{RF}, at Larmor frequency, $\boldsymbol{\omega_L}$, and this will generate an oscillating RF field (Figure 4) [18].

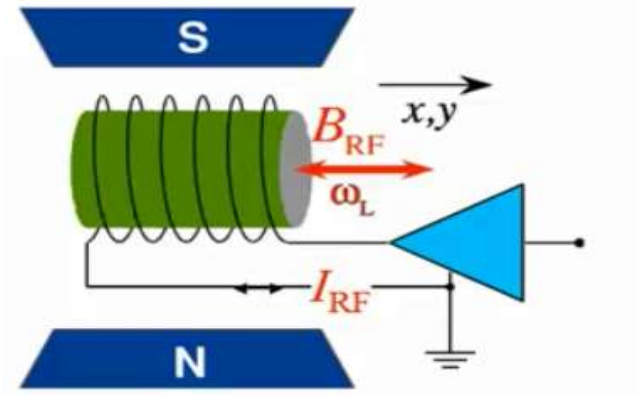

Figure 4: Schematic of a transmitter and a transmit amplifier connected to it.

The efficiency of the transmitter can be enhanced by increasing the number of turns of the wire and reducing the diameter of the coil, so that the turns of the wire will be closer to the NMR spins within the patient. So if the coil is more tightly close to the patient, the SNR will be increased. The numerical expression representing the efficiency of the transmitter (figure of merit) is

$$B_U = \frac{\boldsymbol{B_1}}{\boldsymbol{I_{RF}}} \quad \textbf{(}\text{equation 2)}$$

where B_U is the transmit efficiency (field/unit current).

Reciprocity: The law of reciprocity relates to the transmit and receive properties of the RF coil. This can be expressed as:

$|\xi| = \omega_L \mathbf{m_{xy}}.\ B_U\ [\omega_L \mathbf{m_{xy}}$ (receiver) $\alpha\ B_U$ (transmitter)] **(**equation 3)

where m_{xy} is the transverse component of the rotating magnet moment, B_U is the RF coil's efficiency (field/unit current) and ω_L is the precession frequency. The preceding expression links the coil's behaviour as a transmit coil to its behaviour as a receive coil. A RF coil which is an efficient transmitter is also a sensitive receiver [8].

Materials and Methods

This is an experimental research conducted at Biomedical Laboratory using 0.2T FFC-MRI machine at University of Aberdeen. It describes the modelling and design methodology applied for constructing the various RF coils as well as the procedures followed to obtain the value of the intrinsic properties of the coils.

Circular loop (CL) surface coil design using copper wire.

The coil design is made up of conducting copper wire and capacitors. The circular loop (CL) surface coil is built with three turns of copper wire, one on top of each other with a diameter of 10cm. A capacitive matching circuit (tuning and matching capacitors) was adopted to adjust the impedance to fifty Ohms (50Ω).

The tuning capacitor was connected between two ends of the copper wire while the matching capacitor was connected between the copper wire and the co-axial cable that connected the coil and the network analyser. This RF coil design generates B_1 field that is perpendicular to the coil plane (axial B_1 field) in the central region of the coil and the amplitude decreases along the coil axis [19].

The axial B_1 field produced by this coil is suitable for MRI systems with horizontal B_0 field. The tuning and matching variable capacitors were adjusted such that the resistance was 50Ω and the reactance was zero. The CL prototype was finally tuned to 8.4 MHz suitable for a 0.2 T magnet system.

Circular loop (CL) surface coil design using litz wire.

Litz wire is a conductor comprising a bundle of multiple insulated strands, woven together in such a way that there is even distribution of current among the separated strands and all the strands pass through all points within the conductor, which reduces the effect of eddy current.

According to litz wire theory, the total AC resistance is determined by both the strand wire gauge and the number of strands. The AC resistance must be minimised in order to minimise the coil resistance [20]. The functions [*F (x)* and *G (x)*] given by AC resistance per unit length of a litz wire segment can be expressed as:

$$R_{ac} = R_{dc} \cdot \left[\frac{1+F(x)}{s} + \frac{2.s.d^2}{D^2} \cdot G(x)\right]$$

$$x = \frac{d}{\sqrt{2\delta}} \quad \text{(equation 4)}$$

where R_{ac} is the alternating current resistance of a single strand, R_{dc} is the direct current resistance of a single strand, s is the number of strands, d is the diameter of a single strand, and D is the overall diameter of the litz wire and δ is the skin depth, which depend on the frequency. The function *F (x)* is the losses due to skin effect and *G (x)* is the losses due to proximity effect.

In order to avoid skin depth problems, the strands are insulated and braided from each other, otherwise all the wires in the bundle will behave like a single large wire. Another advantage of weaving the litz wire is that the directions of the magnetic field produced by the current flowing in the strands have a reduced tendency to produce an opposing electromagnetic field in the adjacent strands.

The CL surface coil design is made up of litz wire and capacitors. The CL surface coil is built with three turns of litz wire with 2mm spacing between the loops and the diameter of the coil is 10cm. The litz wires were six, braided together and the insulators of both ends of the wire connecting the capacitors were properly burnt using a soldering iron in order to make it a good conductor. The capacitive matching circuit was carried out to adjust the impedance to 50Ω. The tuning capacitor was connected between the two ends of the litz wire while the matching capacitor was connected between the litz wire and the co-axial cable that connect the coil and the RF network analyzer.

This RF coil design also generates an axial B_1 field in the central region of the coil, which is suitable for MRI systems with horizontal $\boldsymbol{B_0}$ field (Figure 5). The tuning and matching variable capacitors were adjusted until the resistance of the coil becomes 50Ω and the reactance becomes zero.The CL prototype was finally tuned to 8.4 MHz suitable for a 0.2 T magnet system.

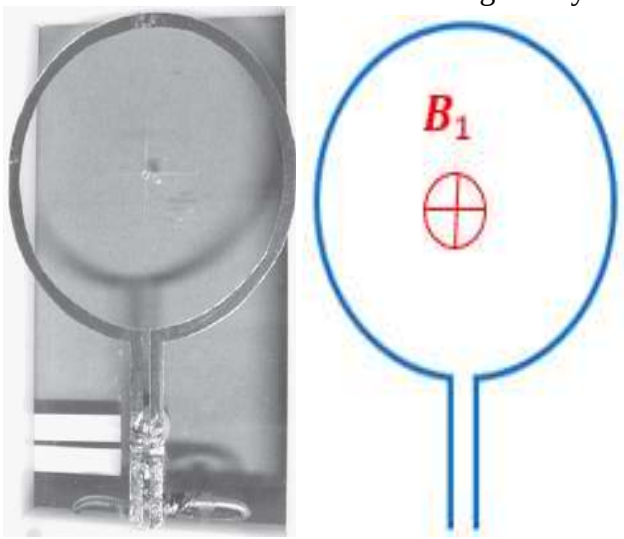

Figure 5: Schematic design and prototypes of CL RF coil tuned to 8.5 MHz and used for FFC - MRI testing with phantoms. The diameter is 2R = 10 cm.

Birdcage Coil design

This is the last coil design that was attempted and which was used as ~~the~~ transmitter coil that will excited the nuclear spin of the sample. The receiver surface coil will depict the voltage signal from the transverse magnetisation. Initially, a previously existing high pass birdcage coil was used during the experimental procedure in order to farmiliarise with the tuning and coupling methods involved in the coil design and also to compare the field homogeneity with the modified version of same coil about to be designed. The type of birdcage coil used for this experiment had a high-pass configuration, with the capacitance placed on the end rings as shown in Figure 6.

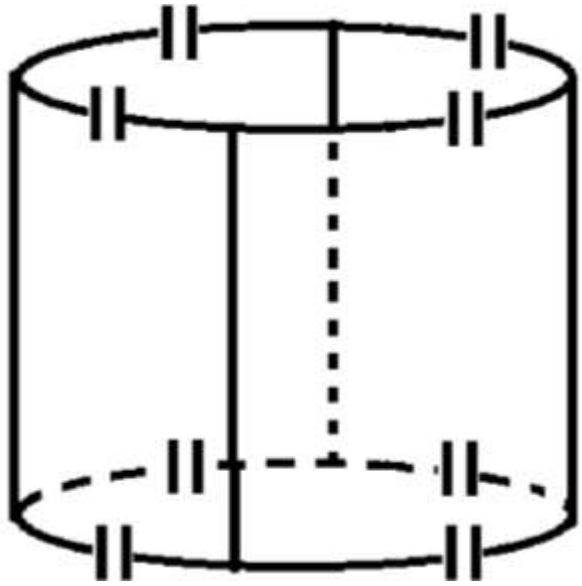

Figure 6: High-pass birdcage coil. The capacitors are placed on the end rings.

The coil had eight legs and sixteen capacitors (3.1 nF) placed on the end rings and B_1 field measurements were taken. The coil was later modified by increasing the number of legs to sixteen and the capacitance (6.5 nF) to thirty-two. The rationale behind adding the number of legs in the coil is to increase the field homogeneity because in a birdcage coil design, the higher the number of legs, the more the field homogeneity (Figure 6).

Quality factor

The quality factor is one of the major intrinsic parameters of the coil that needs to be recorded because it determines the coil's efficiency as a transmitter, and the sensitivity as a receiver. The RF network analyser also provides the means of measuring the quality factor of the resonator. After the tuning and matching of the RF coil impedance to that of the transmission line using Smith chart, the "Notch" function from the "Marker Search" menu is selected and the value of the quality factor will be displayed (Figure 7).

Figure 7: Image display of an RF network analyser used for this experiment. A coaxial cable connecting the RF probe to the reflection mode of the network analyser is also displayed. On the upper left edge is a display of the resonant frequency and the corresponding attenuation. The lower marker represents the maximum attenuation.

Radiofrequency network/signal analyser

This is a test equipment used to measure the response of devices at certain radiofrequencies. In this experiment, it was used to measure the intrinsic parameters of the RF coils, such as the resonance frequency (Hz), the impedance (Ω) and the quality factor.

RF coil uniformity and field homogeneity

The use of a search coil is the most direct and accurate way of measuring B_1 field at frequencies of up to 300MHz. The search coil has a square loop 5mm on each side, directly attached to an RG 174 coaxial cable [19]. The cable is connected to a network analyser via a co-axial cable of 50Ω transmission line (Figure 8).

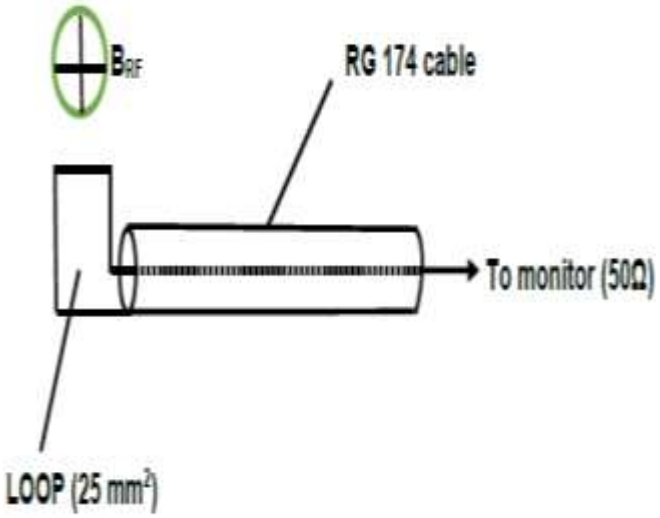

Figure 8: Schematic diagram of a search-coil field probe used for B_1 measurement in this experiment.

The measurement of the B_1 value of a 50Ω system can be performed by applying the formula

$$\boldsymbol{B_1} = \frac{5\alpha}{\omega A} \qquad \textbf{(}\text{equation 5)}$$

Where ω is the angular frequency (measured in radiance per second), A is the search loop area, which is equal to 25 mm^2 (A= $25mm^2$) and α is the round-trip attenuation ratio, which can be expressed as:

$$\alpha = 10^{-[(\text{atten. in dB}/20]} \qquad \textbf{(}\text{equation 6)}$$

The negative sign in the formula above indicates the attenuation in the material [19].

Skin depth

As the frequency is increased, the current fall-off exponentially with increasing skin depth. As shown in figure 11, when the frequency is at 1 MHz, the current flow along the RF tube rather than the continuous cross sectional area (DC) and to calculate the effective cross sectional area carrying of the RF current, this formula: $A = 2\pi r^2\delta$ is used instead of $A = \pi r^2$ [8].

The skin depth δ is given by

$$\delta = \sqrt{\frac{2}{\mu_0 \omega \sigma}} \quad \text{(equation 7)}$$

where $\mu_0$is the magnetic permeability ($\mu_0 = 4\pi \times 10^{-7}$ H/m), σ is the wire conductivity. The skin depth in copper is about 66 µm at 1 MHz.

The proximity effect arises when the copper wire is bent into a coil, which result to further increase in RF resistance.

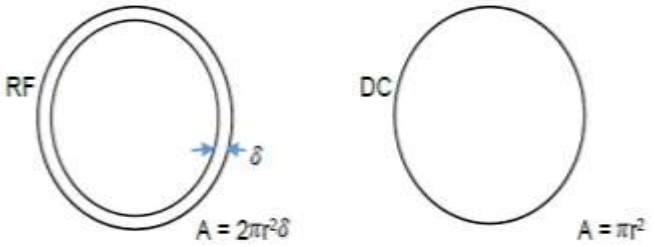

Figure 11: Schematic of skin depth effect on RF copper tube compared to a circular wire.

Results

This chapter presents the outcome of the designing procedure of the CL surface coils and the volume coil as well as the measurements obtained regarding the intrinsic parameters of each coil.

Development of the first surface coil using copper wire

These was the first coil constructed at the initial stage of this experiment in order to get farmiliarise with the procedure of how the coil is designed and its functionality. Also to farmiliarise with how to use the network analyser as a guide to carry out the procedure. The coil was deigned on a plastic material, with three turns of copper wire. The main intrinsic parameter of the coil was measured.

After the tuning and matching of the coil using variable capacitors, the following values were obtained in table 1.

Development of the main CL coil using copper wire

The constructed CL coil was connected to the network analyser via a coaxial cable. Using a search loop with exact configuration described in Figure 8, the value of B_1 field measurement was obtained using equation 5 and 6. Table 2 presents the calculated values of the B_1 measurement at various distances and figure 9 shows the graphical presentation of the values obtained.

During the process of constructing the coils other important intrinsic parameters such as the resonant frequency and the quality factor were obtained, as shown in the table. After the tuning and matching of the coil using variable capacitors, the following values were obtained in table 3.

Development of CL coil using litz wire

The same procedure was adopted exactly the same as CL coil using copper wire described above and table 4 presents the calculated values of the B_1 field measurement at various distances and figure 10 shows the graphical presentation of the values obtained.

Development of the birdcage coil

As discussed earlier, the previously existing high pass bird cage coil had eight legs and sixteen capacitors of 3.1 nF placed on the end rings and the intrinsic parameters was taken before the coil was modified. The values of the intrinsic parameters of the coil are shown in table 5.

The coil was later modified by increasing the number of legs to sixteen and the capacitors (3.1 nF) to thirty-two as shown in table 6. Table 5 shows the intrinsic parameters obtained during the tuning and matching of the modified birdcage coil, the desired resonant frequency was achieved.

Table 1: The obtained values of the main parameters of the surface coil as displayed on the screen of the network analyser

Surface coils	*f* (MHz) of the coils	Q factor
Circular Loop	8.362	47.1

Table 2: The values of B_1 field measurement of CL coil using copper wire at various distances

Distance (cm)	Maximum attenuation (dB)	B_1 field measurements (nT)
2	82.1	297.4
4	83.8	244.6
6	87.2	165.3
8	89.4	128.4
10	93.4	81.0

Table 3: The value of the resonant frequency and the quality factor obtained from the CL coil using copper wire as displayed on the screen of the network analyser

Surface coils	*f* (MHz) of the coils	Q factor
Circular Loop	8.462	85.7

Table 4: The values of B_1 field measurement of CL coil using litz wire at various distances

Distance (cm)	Maximum attenuation (dB)	B_1 field measurements (nT)
2	85	213
4	89	134.4
6	91	106.8
8	95	67.4
10	99	42.5

Table 5: The intrinsic parameter of the previously existing birdcage coil

f (MHz) of the coils	Q factor
8.42	8.462

Table 6: The various capacitors used and the resultant resonant frequency during the birdcage coil design

Capacitors (nF)	***f* (MHz)**
4.7	9.1
5.1	8.7
6.5	7.1
10.3	5.6

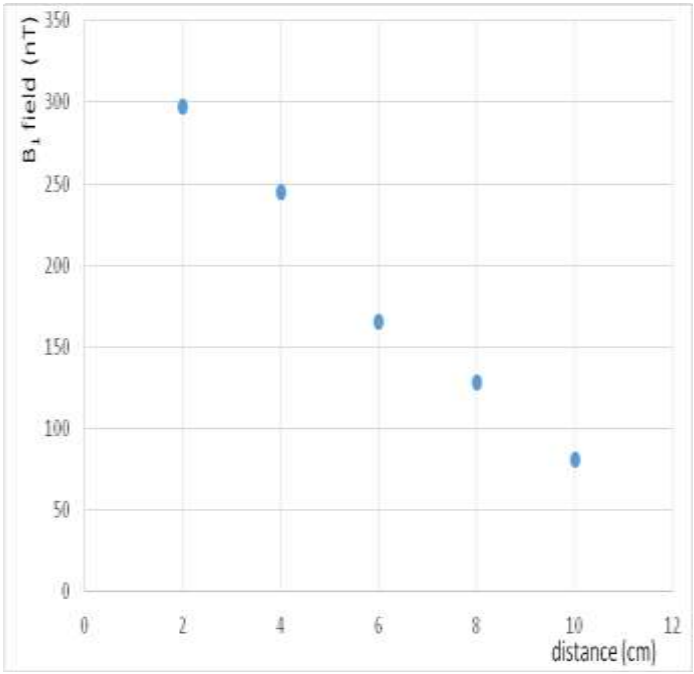

Fig 9: The graphical presentation of the values of B_1 field measurement of CL coil using copper wire at various distances.

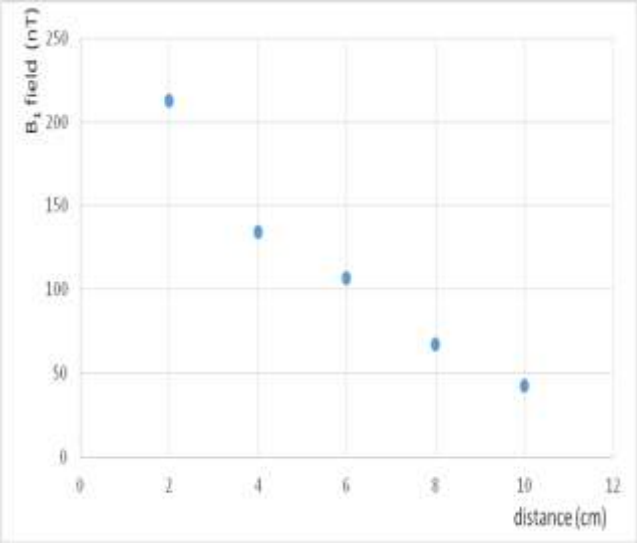

Fig 10: The graphical presentation of the values of B_1 field measurement of CL coil using litz wire at various distances.

Discussion

The CL RF - receive surface coil and a birdcage RF - transmit volume coil were tuned to 8.5 MHz (0.2 T) suitable for FFC-MRI testing. Capacitive matching was adopted for the CL RF coil using both tuning and matching capacitors while inductive matching was adopted for the birdcage RF coil using a coupling loop. Both matching and tuning of the coils were under the guide of RF network analyser.

The birdcage transmitter coil was used to excite the nuclear spins of the sample (phantom) while the CL receiver surface coil was used to depict the voltage signal from the transverse magnetisation. A spoiled gradient echo (GRE) and unspoiled gradient echo pulse sequences were used to acquire images of a cylindrical (12 cm diameter) phantom containing 100 ml of physiological saline and positioned at about 2 mm from the RF coil plane.

The acquisition parameters for both spoiled and unspoiled GRE were: Echo time (TE) = 4ms and Repetition time (TR) = 33ms, slice thickness 2 mm, slice spacing 5 mm, FOV = 16 cm x 16 cm with flip angle (α) = 30^0.

The SNR and the image acquisition time obtained using CL coil constructed with litz wire was higher compared to that constructed with copper wire. The reason is because copper wire suffers a phenomenon known as skin depth (the restriction of RF current flow near the surface of a conductor).

Conclusion

This research was aimed at developing and optimising a series of RF-receive surface coils and RF-transmit volume coil suitable for a 0.2 T FFC-MRI system. The design process included the construction and optimisation of a CL RF coils and a birdcage RF coil. For each of the coils, various measurements were obtained to determine their intrinsic parameters. Three types of CL RF coils were constructed. The first and second construction involved the use of copper wires while the third one involved the use of litz wire.

Also the CL coils were constructed in three turns with a diameter of 100mm. The RF coils were tuned to 8.5 MHz and the $\boldsymbol{B_1}$ field measurements were obtained. The quality factors of all the constructed coils using network analyser and a search-coil field probe were also measured. Bench testing of the coils showed promise as receiver coils for the FFC-MRI system. The images of a phantom containing 100 ml of physiological saline were obtained but the noise and artefact of the copper wire constructed CL coil was significant while the litz wire constructed CL coil showed improved SNR.

References

1. Abragam A. The Principles of Nuclear Magnetism, Oxford University Press, Oxford, 1961; 4-5.

2. Brunner D.O., Zanche N.D., Fröhlich J., Paska J., Pruessmann K.P. Travelling-wave nuclear magnetic resonance. *Nature*, 2009; 457 (1): 994-998.

3. G. Ferrante G., Sykora S. Technical aspects of fast field cycling, *Adv.Inorg.Chem*, 2006 57 (3) :405-470

4. Lurie D.J., D.M. Bussell D.M., L.H. Bell L.H., Mallard J.R. Proton-electron double magnetic resonance imaging of free radical solutions. *J.Magn.Reson*., 1988; 76 (2): 366-370.

5. Lurie D.J., Broche L.M., Choi C.H., Davies G.R., Ismail S.R., O Hogain D., Pine K.J. Fast Field-Cycling Magnetic Resonance Imaging. Ampere NMR School. Wierzba, Poland, 2010; p. 37.

6. Lurie D.J., Broche L.M., Davies G.R., Payne N.R., Ross P.J., Zampetoulas V. Field-cycling MRI – a curiosity or the next big thing?. AMPERE NMR School, Zakopane, Poland, 2016; p11.

7. Lurie D.J., Aime S., Baroni S., Booth N.A., Broche L.M, Choi C., Davies G.R., Ismail S.R., O Hogain D., Pine K.J. Fast Field-Cycling Magnetic Resonance Imaging.Multiscale. *Comptes Rendus Physique*, 2010; 11 (1):136-138.

8. Woo D.C., Choe B.Y., Ha S.H., Choi C.B. Evaluation of the turn variation of spiral RF surface coils for microscopic imaging and spectroscopy. *Measurement*, 2007; 40 (3):615–622.

9. Doyle V.L., Payne G.S., Collins D.J., Verrill M.W., Leach M.O. Quantification of phosphorus metabolites in human calf muscle and soft-tissue tumours from localized MR spectra acquired using surface coils. *Physics in Medicine and Biology*, 1997; 42 (1): 691–706.

10. Meyerspeer M., Krssak M., Kemp G.J., Roden M., Moser E. Dynamic interleaved 1H/31P STEAM MRS at 3 Tesla using a pneumatic force controlled plantar flexion exercise rig. *Magnetic Resonance Materials in Physics, Biology and Medicine*, 2005; 18 (2): 257–262.

11. Alecci M., Romanzetti S., Kaffanke J., Celik A., Wegener H.P., Shah N.J. Practical design of a 4 Tesla double-tuned RF surface coil for interleaved 1H and 23Na MRI of rat head. *Journal of Magnetic Research*, 2006; 181 (3): 203–211.

12. Roemer P.B., Edelstein W.A., Hayes C.E., Souza S.P., Mueller O.M. The NMR phased array. *Magnetic Resonance in Medicine*, 1990; 16 (2):192–225.

13. Wright S.M., Wald L.L. Theory and application of array coils in MR spectroscopy. *NMR in Biomedicine*, 1997; 10 (4):394–410.

14. Weiger M., Pruessmann K.P., Leussler C., Roschmann P., Boesiger P. Specific coil design for SENSE: a six-element cardiac array. *Magnetic Resonance in Medicine*, 2001; 45 (2): 495–504.

15. Sodickson D.K., McKenzie C.A., Ohliger M.A., Yeh E.N., Price M.D. Recent advances in image reconstruction, coil sensitivity calibration, and coil array design for SMASH and generalized parallel MRI. Magnetic Resonance Materials in Physics, Biology and Medicine, 2002; 13 (1): 158–163.

16. McRobbie D.W., Moore E.A., Graves M.J., Prince M.R. MRI from Picture to Proton. Cambridge: Cambridge University Press, (2003).175-183

17. Anoardo E., Galli G., Ferrante G. Fast-field-cycling NMR: Applications and instrumentation. *Appl. Magn. Reson*, 2001; 20 (2) :365-404.

18. Alfonsetti M., Mazza T., Alecci M., Optimisation of multi-element transverse field radiofrequency surface coils. *Measurement Science and Technology*. 2006; 17 (1):53-59.

19. Hutchison JMS. Frequency and power considerations for in-vivo EPR and Related techniques. In: BERLINER, L.J., ed., 2003. In-vivo EPR (ESR). Theory and applications. Springer, USA: *Biological Magnetic Resonance* 2003; 18 (3): 41-59.

20. Sullivan C.R., Charles R. Optimal Choice for Number of Strands in a Litz-Wire Transformer Winding. *IEEE Transactions on Power Electronics*, 1999; 14 (2*): 283–291*

How to cite: Abubakar U, Broch L, Ugwu AC, Audu SA, Danfulani M, Mohammed A, Abba M, Miftaudeen NM. Development and optimisation of surface and volume radiofrequency coils suitable for fast-field-cycling magnetic resonance imaging (FFC-MRI). J Rad & Radiat Sci, 2018; 32 (1): 46 - 56